Building Characterisation using Polarimetric Interferometric SAR Data

S. Guillaso*, L. Ferro-Famil†, A. Reigber*, and E. Pottier†
*Technical University Berlin, Department of Computer Vision and Remote Sensing.
Straße des 17. Juni 135, EB9, D-10623 Berlin, Germany. Email: stephane@fpk.tu-berlin.de
†IETR Institute, University of Rennes 1, UMR CNRS 6164, "SAPHIR" team
Campus de Beaulieu – Bât. 11D – 263 Av. Général Leclerc, CS 74205 F-Rennes cedex, France

***Abstract*— This paper describes the characterisation of buildings using fully polarimetric interferometric SAR data at L-band. This analysis is performed in two steps. Urban targets are first discriminated from surrounding natural media, using a polarimetric classification procedure. Then, urban objects are characterised by their shape information. The length and width is obtained using a superresolution procedure. An interferometric phase estimation, based on ESPRIT principle, is applied for the retrieval of the heigth of different media and specifically for the heigth of the buildings.**

I. Introduction

The characterisation of three-dimensional (3-D) structures, like buildings, from complex L-band SAR data is a complex task. Problems arise due to the varying nature of highly spatially concentrated targets like buildings, green areas and infrastructures (roads, bridges...). Normally, X-band SAR data are used for this purpose, but L-band waves have a high penetrability in volume area and it is possible to use this property for building characterisation.

Pratically, the analysis of man-made areas may be decomposed into two steps: detection of the different types of contributors as well as the extraction of their geometrical parameters. The detection step performs a discrimination of man-made targets from surrounding natural media, present on the scene, using a polarimetric segmentation. The principle is described in part II.

In order to improve the result of the polarimetric segmentation, it is necessary to inhence the resolution of the L-band SAR images. In the airborne case, due to the variation of the incidence angle, the wavenumber shift [1] between the two images is not constant over range. In part III, a range resolution enhancement algorithm is presented, which takes into account locally varying wavenumber shifts. By this approach, results of classification give a better discrimination of the double bounce class, which is use to localise the edge of buildings.

A high-resolution method is used for the determination of dominant local scatterers and the estimation of the corresponding interferometric phases. This approach is based on ESPRIT algorithm and usually employed for direction of arrival (DoA) estimation on an antenna array. Here, this approach is used over built-up areas, in order to estimate the nature of the different scattering mechanisms and recover phase corresponding to the top of building. Then, the height is recovered using classical interferometric phase analysis.

The efficiency of this three-dimensional built-up area structure extraction is demonstrated using fully polarimetric multi-baseline SAR images, obtained from DLR-ESAR airborne sensor in L-band repeat-pass mode.

II. Polarimetric Classification

A classification based on a physical interpretation of scattering is necessary in order to identify the different media present on the scene. This segmentation is applied to single POLSAR data.

A. Unsupervised Wishart H-A-α segmentation scheme

In a monostatic configuration, the sample coherency matrix is define from the element of the scattering matrices as:

$$[T] = \langle \vec{k}\vec{k}^{\dagger} \rangle \text{ with } \vec{k} = \frac{1}{\sqrt{2}}[S_{HH}+S_{VV}, S_{HH}-S_{VV}, 2S_{HV}]^T \tag{1}$$

where $\vec{k}$ is the target vector. For homogeneous areas, the n-look coherency matrix, $[T]$, follows a complex Wishart density function, $W_C(n,\Sigma)$ from which it is possible to define a Maximum Likelihood (ML) classifier [2] which assigns to each pixel of the SAR image a class X_m minimising the following distance:

$$d([T], X_m) = \ln \mid [\Sigma_m] \mid + \text{tr}([\Sigma_m]^{-1}[T]) \tag{2}$$

where $[\Sigma_m]$ is the mean covariance matrix of the class X_m. The unsupervised Wishart H-A-α segmentation scheme consists in the iterative k-mean clustering procedure using the ML distance defined in (2). The initialisation of the segment centres in the coherency matrix space requires the use of the polarimetric indicator H (entropy), A (anisotropy) and α, derived from an eigendecomposition of the sample coherency matrix $[T]$.

B. Data Set Characterisation

The estimation of the nature of the scattering mechanism is given by an interpretation of the polarimetric indicator. H indicates the random aspect of the global scattering phenomenon, A denotes the relative importance of the two secondary scattering mechanisms, and α indicates the nature of the scattering mechanism. It varies from 0, corresponding to a isotropic surface to 90 indicating a isotropic dihedral or helix. In [2],

[3] the procedure of the segmented H-A-α characterisation is presented.

This allows to segment data into 3 main categories: double bounce (may indicate the presence of buildings), single bounce (surface reflection), and volume scattering (e. g. forest area).

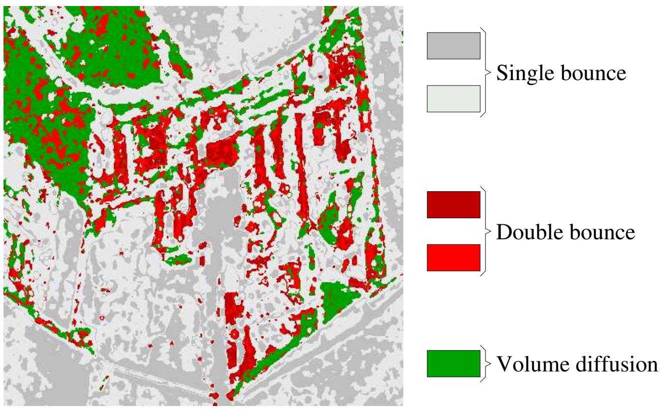

Fig. 1. POLSAR dataset segmented using Unsupervised Wishart H-A-α classification.

Fig. 1 shows segmentation results after applying a Wishart H-A-α classification and the characterisation described in [2], [3]. The red zones indicate double bounce, which designates the presence of buildings and are located at the same place than buildings. However, some building groups are identified as forested area and some vegetation parts are seen as double bounce.

III. Superresolution SAR

The use of the superresolution principle and the high resolution method is helpful to improve the detection and characterisation of building. The superresolution principle is use in order to improve the range resolution and thus to improve the double bounce classification scheme. The use of high resolution method allows the estimation of interferometric phase of different main scattering mechanisms, and then to identify building from surrounding. These two approaches are presented in the following sections.

A. Introduction

The spectra of two SAR images obtained from slightly different look angles contain different parts of the ground reflectivity spectrum. This effect is known in SAR interferometry as ”wavenumber shift” [1]. The basic principle of superresolution is to combine coherently the different parts of the measured spectra, in order to increase the total bandwidth. In this way, an image with enhanced range resolution can be obtained.

Due to the variations of the incidence angle, in the airborne case, the wavenumber shift between the two SAR images is not constant over range. Consequently, this means that the possible resolution enhancement is range dependant. In the following, a range adaptative algorithm is described, which takes into account locally wavenumber shifts.

B. The principle of the superresolution

The range resolution of a SAR image is given by:

$$\delta_r = \frac{c}{2W} \tag{3}$$

with W represents the range bandwidth and c is the speed of light. Thus, the resolution improvement needs to increase the effective bandwidth W. Like the bandwidth is governed by the system, this value cannot be change during data acquisition. The idea of the superresolution is now to determine an increased bandwidth of the ground reflectivity spectrum, by combining two spectra of images obtained with a slightly different incidence angle. In tha airborne case, the spectral shift is strongly range dependant and a spectral adjustement is necessary before both spectra can be joined.

C. The superresolution algorithm

The superresolution algorithm for the airborne case consists out of two steps. The first step is a range dependant spectral shift, in order to align the spectra of both images. The second step is a spectral combination, in order to form a superresolution image with increased bandwidth. A schematic overview of this algorithm is shown in Fig. 2.

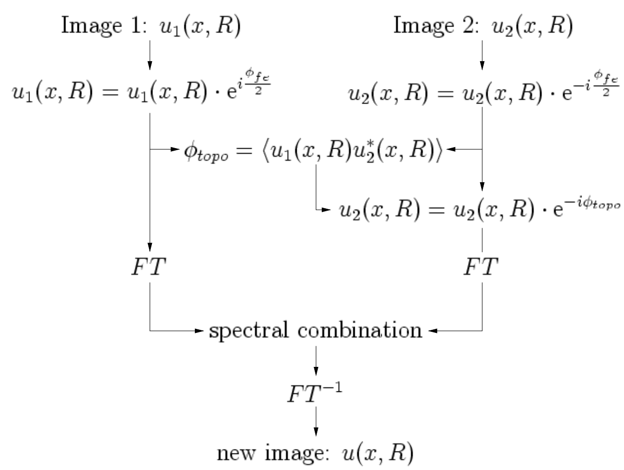

Fig. 2. Block diagram of the proposed superresolution algorithm.

As it is known from literature, the amount of spectral shift in the frequency domain corresponds to the range frequency of the interferometric phase in the time domain [1]. Neglecting topographic effects, the interferometric phase is equal to the flat-earth phase correponding to the processed reference plane. In the airborne case, its shape is strongly curved, following:

$$\phi_{fe}(r) = \frac{4\pi}{\lambda}(R_1(r) - R_2(r)) \tag{4}$$

where ϕ_{fe} is the flat-earth phase and $R_1(r)$ and $R_2(r)$ denote the slant-range distances between the sensor and a target located at the respective range r. The curvature of the flat-earth phase thereby reflects exactly the range dependence of the spectral shift. In range compressed data, the impulse responses are well located and it becomes approximately correct to associate every range-bin a local spectral shift, given by the deviation of the flat-earth phase. This derivation can be assumed to constant over the extent of an impulse response, as the flat-earth phase is a slowly varying function. By multiplying one of the complex SAR images by $\exp(i\phi_{fe}/2)$ and the other by $\exp(-i\phi_{fe}/2)$, a spatially varying frequency shift compensation in the frequency domain is applied symmetrically on both images. After this operation, all target spectra are aligned, independently of their range position [4]. The use of the flat-earth phase instead of the real interferometric phase for compensating the spectral shift neglects influences of the topography on the local incidence angle and, therefore, on the local spectral shift. To compensate this error, an additional phase correction has to be applied on one of the images. The required phase function is the residual topographic phase, ϕ_{topo}, whose "wrapped" form can be estimated by forming the interferogram between the two images after spectral shift compensation.

The second part of the algorithm is the spectral combination of both images. To avoid sudden jumps in the final spectral, it is helpful to use a continuously characteristic filter, which is calculated from the overlap of the two ground reflectivity spectra. This filter ensures a smooth transition from one spectrum to the other, while information coming from the uncorrelated part are not affected.

D. Results

The algorithm described above is applied to L-band repeat-pass fully polarimetric data of the Oberpfaffenhofen/Germany test site, acquired by DLR's E-SAR airborne sensor. The two passes have an average horizontal and vertical baseline of 240,8 m and 0,5 m, respectively. A new superresolution image is formed in each initial polarisation channel (HH, HV, VH, VV). From this new data set, a polarimetric segmentation is performed. Fig. 3 shows the double bounce area from superresolution images. On this image, the building edge are well located by their L-form. Using superresolution principle, the building shape retrieval is significantly improved.

IV. Phase Estimation Using ESPRIT Approach

Backscattered waves result from the sum of contribution corresponding to different scattering mechanisms. Depending on the nature of the obseved medium, the value of the resulting interferometric may vary in a significant way. The use of the ESPRIT technique permits to separate the different scattering mechanisms and to estimate the main interferometric phase.

The signals acquired during an interferometric measurement, s_1 and s_2, may be written as:

$$
\begin{aligned}
s_1^{pq} &= \sum_{m=1}^{d} \sigma_m \zeta_m^{pq} \mathrm{e}^{i\frac{4\pi}{\lambda}R} + n_1^{pq} \\
s_2^{pq} &= \sum_{m=1}^{d} \sigma'_m \zeta_m'^{pq} \mathrm{e}^{i\frac{4\pi}{\lambda}(R+\Delta R_m} + n_2^{pq}
\end{aligned} \quad (5)
$$

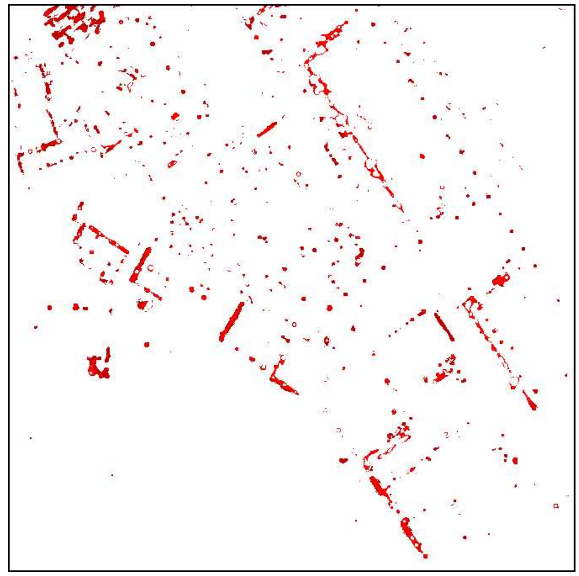

Fig. 3. Double bounce area (superresolution data)

where pq denote the polarisation channel (HH, HV, VH, VV). These signals consist of a sum of d different elementary scattering contributions represented by ζ_m^{pq} and $\zeta_m'^{pq}$ denoting the normalised backscattering coefficients of the m-th local scatterer in the pq polarisation, and σ_m and σ'_m denoting the intensity of the m-th local scatterer. R is the slant range distance from the master orbit. ΔR_m is the range difference of the m-th scatterer between master and slave tracks. Finally, n_m^{pq} denotes additive Gaussian noise in the pq polrisation channel. Using a matrix and vector notation, (5) may be written as:

$$
\begin{aligned}
&\vec{s}_1 = [A]\vec{\sigma} + \vec{n}_1 \text{ and } \vec{s}_2 = [A']\vec{\sigma}' + \vec{n}_2 \\
&\text{with } \vec{s}_{1,2} = [s_{1,2}^{HH}, s_{1,2}^{HV}, s_{1,2}^{VH}, s_{1,2}^{VV}]^T
\end{aligned} \quad (6)
$$

In the case of sufficiently small baselines, scattering coefficient of each local scatterer for both interferometric acquisitions are assumed to be remain identical: $\zeta_m^{pq} = \zeta_m'^{pq}$, $\sigma_m = \sigma'_m$. Then, $\vec{s}_2$ may be simplified as follows:

$$\vec{s}_2 = [A][\Phi]\vec{\sigma} + \vec{n}_2 \text{ with } [\Phi] = \mathrm{diag}\{\mathrm{e}^{i\phi_1}, \mathrm{e}^{i\phi_2}, \cdots, \mathrm{e}^{i\phi_d}\} \quad (7)$$

The form of (6) and (7) are adapted to the TLS-ESPRIT algorithm. Thus, the interferometric phase of each dominant scatterers can be estimated from $[\Phi]$ (see also [5], [6]).

A. Application to SAR data

The ESPRIT approach is applied on L-band repat-pass fully polarimetric data of the Oberpfaffenhofen/Germany test site, acquired by DLR's E-SAR airborne sensor. The two passes have an average of 6 m baseline.

Fig. 4 shows an optical image of the test site. (1) indicate the building under study.

Fig. 4. Optical image of the Oberpfaffenhofen test site.

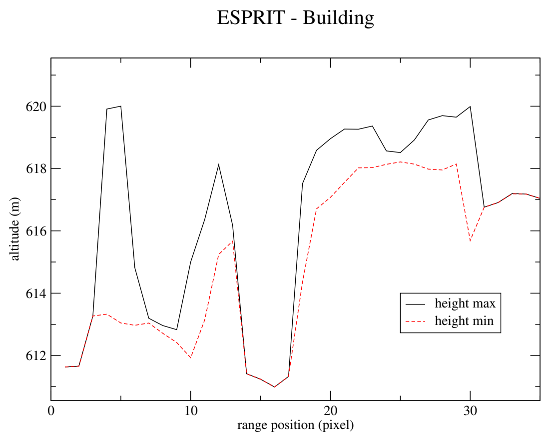

Fig. 5. Estimated height over the building under study.

Fig. 5 shows the estimated height profile provides using ESPRIT approach after phase to height conversion. The behaviour of the height profile indicates the nature of the target. In the area under study, there are 2 targets, trees (A and B) and a building (C). The estimated height reaches a same value over the building whereas these values are different over trees. Using this statement, it is possible to localise the position of buildings, and using estimated height information, a 3-D images of buildings is shown by Fig. 6. On this representation, all vegetal information is removed, only surface and building information is keeped. The building groups ($1 \rightarrow 5$) are well defined. Fig. 7 represents the ground truth using a optical image with the localisation of the building groups.

V. Conclusion

This paper presents a building characterisation using L-band interferometric polarimetric SAR data by two approaches. The shape and orientation is given using a superresolution algorithm and a polarimetric segmentation. This superresolution method improves the range resolution of the data and permits to get a better accuracy for the polarimetric segmentation. The localisation and the height extraction is given by the use of ESPRIT method. This approach gives two estimated phase of dominant scattering mechanisms which are used to give better accuracy in height extraction.

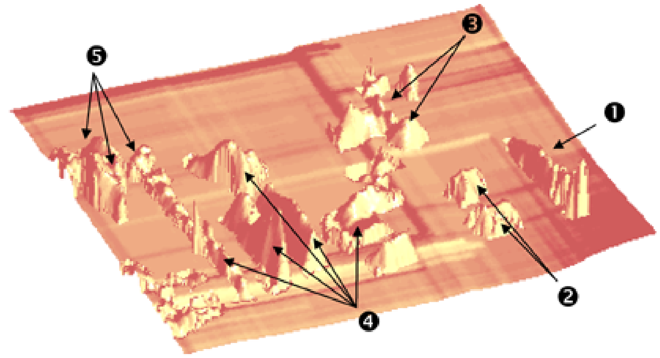

Fig. 6. 3-D representation of buildings.

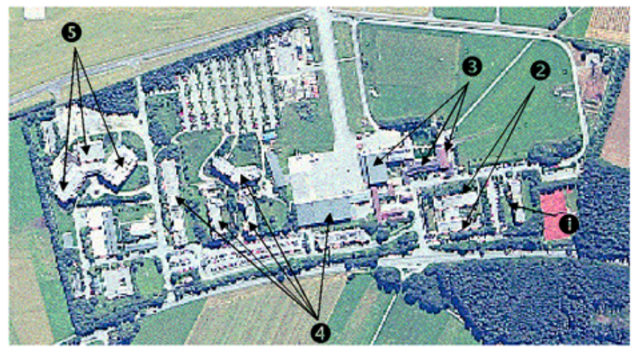

Fig. 7. Optical image of the test site.

References

[1] F. Gatelli, A. M. Guarneri, F. Parizzi, P. Pasquali, C. Prati and F. Rocca, *The Wavenumber Shift in SAR Interferometry*, IEEE Transactions on Geoscience and Remote Sensing, Vol. 32, No. 4, pp. 855-864, July 1994.

[2] L. Ferro-Famil, E. Pottier, and J.S. Lee, *Unsupervised Classification of Natural Scenes from Polarimetric Interferometric SAR Data*, Frontiers of Remote Sensing Information Processing, C.H. Chen chief editor, World Scientific Publishing, 2003.

[3] L. Ferro-Famil, E. Pottier, and J.S. Lee, *Classification and Interpretation of Polarimetric Interferometric SAR data*, Proceedings IGARSS'02, Toronto, 2002.

[4] A. Reigber, *Range Dependent Spectral Filtering to Minimize the Baseline Decorrelation in Airborne SAR Interferometry*, Proceedings IGARSS'99, pp. 1721-1723, Hamburg, 1999.

[5] S. Guillaso, L. Ferro-Famil, A. Reigber, and E. Pottier, *Analysis of Built-Up Areas from Polarimetric Interferometric SAR Images*, Proceedings IGARSS'03, Toulouse, 2003.

[6] R. Roy and T. Kailath, *ESPRIT – Estimation of Signal Parameters via Rotational Invariance Techniques*, IEEE Transactions on Acoustic Speech Signal Processing, Vol. 37, No. 7, pp. 984-995, July 1989.